Comparative thermal analysis of an advanced ceramic-coated piston in a spark ignition engine**

Jai Kumar Sharma* and Ritu Raj

Department of Mechanical Engineering, ITM University, Gwalior, Madhya Pradesh (M.P.), India

This study deals with the steady-state temperature variation in the partially ceramic-coated Al–Si piston of a petrol engine investigated using ANSYS Workbench finite-element modeling software. The ceramic material used for coating the piston crown was lanthanum cerate ($La_2Ce_2O_7$). Coating width and thickness effects were explored and compared with an uncoated piston. Convection boundary conditions were considered. The coated surface temperature is greater than that of the uncoated piston and increases with increasing coating thickness, while normal stress decreased.

Keywords: ceramic coating, finite element modeling, internal combustion engine, lanthanum cerate, thermal barrier coating

1. Introduction

Nowadays, improvement of total efficiency and performance of spark ignition (SI) engine components, internal combustion (IC) engine components and gas turbines are achieved using thermal barrier coatings (TBCs) [1–5]. They have also been used in adiabatic engines, lowering heat rejection and failure fatigue of the inner metallic surfaces while also reducing harmful emissions [6–10]. A TBC consists of several layers, viz. successively a substrate, an intermediate bond coat layer and a top ceramic coating consisting of lanthanum cerate [11, 12]. As well as hindering heat transfer (heat flux), TBCs also protect the piston from corrosive attack [13–16]. Better utilization of the energy carried by the exhaust increases the work done inside the cylinder [8, 15, 17].

Hence, in SI engines the use of TBCs leads to improvements in performance and efficiency and, furthermore, a decrease of harmful exhaust emissions from the engine [18–22]. In the present analysis, a partial ceramic coating was applied to the piston of a SI engine. In previous research [19], hydrocarbon (HC) emissions beginning from a cold start of a standard (uncoated)

* Corresponding author. E-mail: jaikumarsharma94@gmail.com

** This paper was first presented at the International Conference on Advanced Materials, Energy & Environmental Sustainability (ICAMEES-2018), 14–15 December 2018 in Dehradun, India.

Received 30 January 2019; *accepted* 31 July 2019

doi: 10.4024/N14SH19A.ntp.15.02

engine were compared with those from engines having partially ceramic-coated pistons. Significant reductions of CO and HC emissions were observed with the coated pistons. A temperature increase of 100 °C at the ceramic-coated surface (coating thickness 0.5 mm) was observed [18, 19].

The topmost ceramic layer decreases the internal stress that arises within the substrate during thermal shock; the coating thickness has a direct effect on the thermal stress. The modulus of elasticity, thermal conductivity and thermal expansion coefficient of the materials are the main factors on which the robustness of a ceramic coating depends during thermal shock [21, 23, 24]. Calculation of the temperature distribution within the piston is important for controlling the deformations and stresses. Thermomechanical analysis contributes to the design of the piston of an SI engine before the actual manufacturing and testing.

2. Construction of partially coated piston

The piston was made from Al–Si alloy. Material corresponding to the thickness and width of the coating was removed from the piston's surface at its circumference. A NiCrAl bond coat was then applied to form a layer of thickness s = 0.15 mm, onto which a lanthanum cerate ($La_2Ce_2O_7$) coating (thickness t) was applied (at the crown of the piston) by plasma spraying, as shown in Fig. 1.

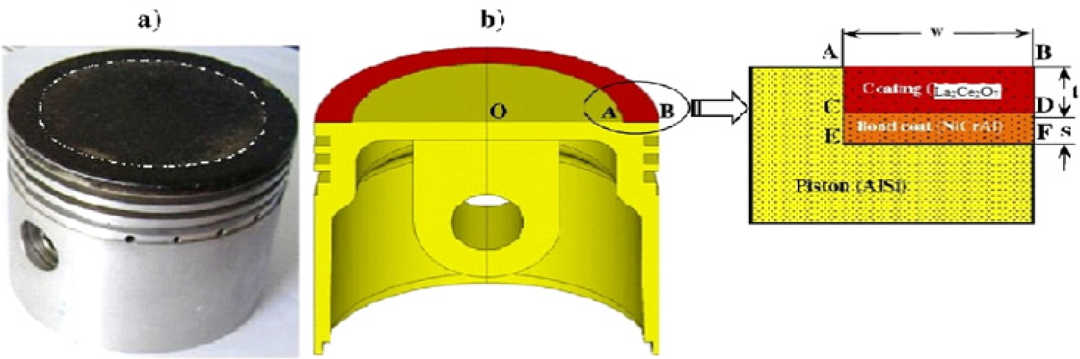

Figure 1. Model for FEM analysis. (a) Photograph of partially ceramic-coated aluminium alloy piston with cast iron rings; (b) cutaway view (half part) of the piston [22]. Inset: width and thicknesses of the TBC applied to the crown of the piston.

3. Thermal analysis

The effects for a petrol engine of the TBC were investigated via steady-state thermomechanical analysis in 3D using ANSYS finite element modeling (FEM) software; a liquid-cooled, single-cylinder SI engine piston was modeled. Widths w and coating thicknesses of the three layers (i.e., the top coat forming the surface, the bond coat and the substrate) are given in Table 1 (cf. Fig. 1b, inset). Specifications of the engine are given in Table 2. Table 3 gives the thermomechanical constants of the different materials used in this analysis. Fig. 2 shows the finite element mesh used for the modeling.

Table 1. Layer thicknesses and widths (cf. inset to Fig. 1b).

t / mm	s / mm	$t + s$ / mm	w / mm
0.15, 0.25, 0.35, 0.45, 0.55, 0.65, 0.75, 0.85, 0.95, 1.05, 1.15, 1.25, 1.35, 1.45	0.15	0.3, 0.4, 0.5, 0.6, 0.7, 0.8, 1.0, 1.2, 1.4, 1.6	9.2
0.35	0.15	0.5	5.2, 7.2, 9.2, 11.2

Table 2. Specifications of the SI engine modeled in this work.

Bore	85.95 mm
Stroke	83.45 mm
Displacement	470.08 mm^3
Compression Ratio	7.4
Power (at 3000 rpm)	45 kW
Maximum speed	3400 rpm

Table 3. Physical constants of the materials used in this work [17, 18, 22, 26–29].

Material (function)	Density / kg m^{-3}	Specific heat / J kg^{-1} K^{-1}	Modulus of elasticity / Gpa	Poisson's ratio	Thermal conductivity / W m^{-1} K^{-1}	Thermal expansion coefficient / K^{-1} × 10^{-6}
Cast iron (piston rings)	7300	460	200	0.30	16	10
AlSi (piston)	2700	960	69	0.33	155	21
NiCrAl (bond coat layer)	7870	764	90	0.27	16.1	12
$La_2Ce_2O_7$ (ceramic top coating)	6290	430	25	0.29	0.6	12.9

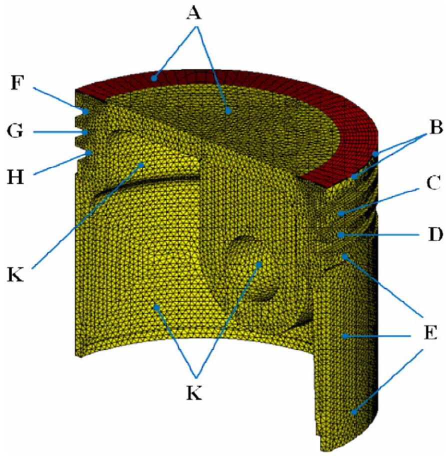

Figure 2. FEM mesh of the cylinder (the letters refer to Table 4).

Convection was selected as the heat transfer mechanism. Heat transfer in SI engines is complex due to the following reasons:

- effects on piston motion arising through neglect of heat transfer;
- possible twisting of the rings (should not occur);
- the piston crown and the rings should be sufficiently oiled to avoid a cavity [14].

Hohenberg proposed the following equation for the instantaneous convective heat transfer coefficient [25]:

$$h_{gas}(T) = \alpha V_C (T)^{-0.06} P(T)^{-0.4} (S_P + b)^{0.8} \quad (1)$$

where V_C, P and T are the instantaneous cylinder volume, pressure and temperature respectively, and S_P is the mean piston speed; α and b are constants. Table 4 gives the boundary conditions applied.

Table 4. Boundary conditions of the piston [22].

Piston region (cf. Fig. 2)	h_{gas} / W m^{-2} K^{-1}	T / °C
A	600	650
B	350	500
C	300	180
D	400	170
E	400	110
F	400	200
G	400	180
H	400	170
K	1500	95

4. Results and discussion

Fig. 3 shows the maximum temperature obtained at the piston crown of both the uncoated piston and coated piston. Maximum temperature of 314.13 °C and minimum temperature of 107.76 °C were obtained for the uncoated piston. Maximum temperature for the partially ceramic-coated piston is obtained with $t + s = 0.5$ mm and $w = 11.2$ mm. The low thermal conductivity of the ceramic material with respect to the aluminium alloy substrate is clearly effective in augmenting the maximum temperature of the piston (preliminary work showed that lanthanum cerate was a better ceramic material then magnesium zirconate due to its lower thermal conductivity). The temperature at the top ceramic-coated surface increases with increase in thickness and width. Radial distance versus ceramic-coated top surface temperature distributions are shown in Fig. 4.

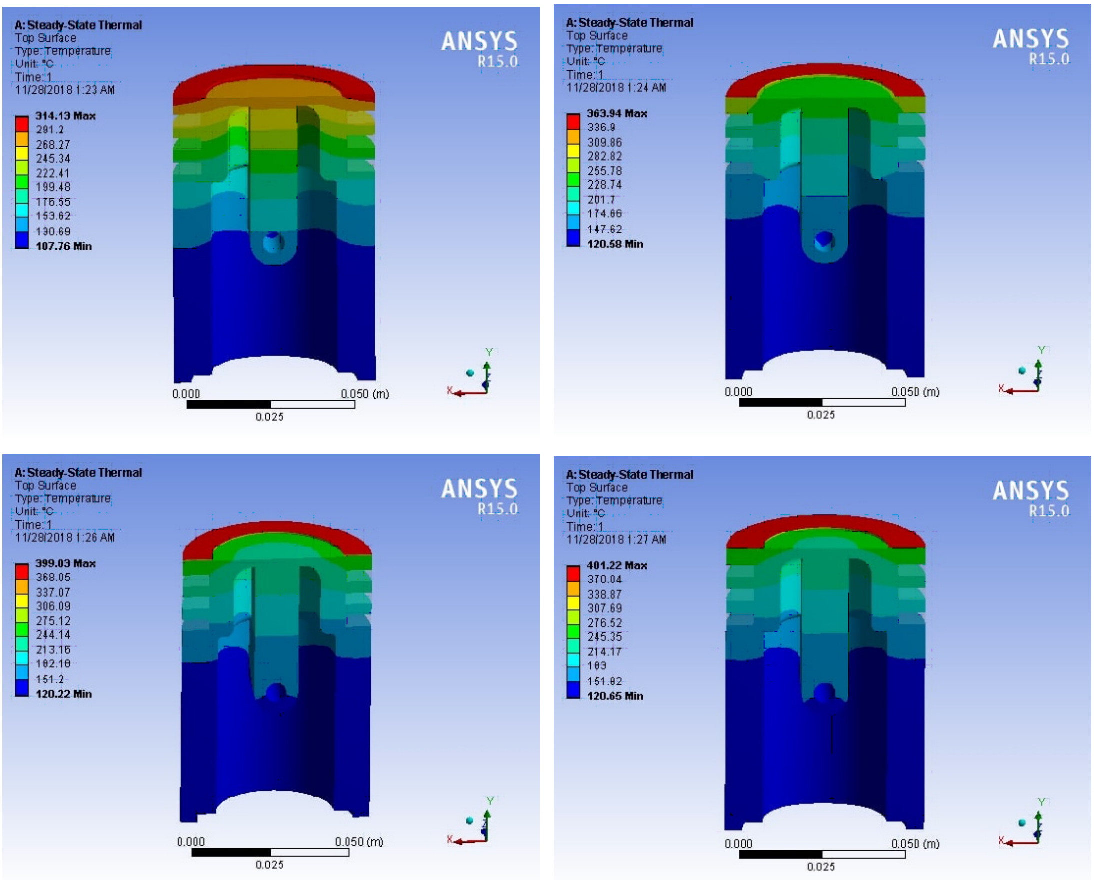

Figure 3. Temperature/°C contours obtained by FEM for the SI engine piston. Top left, uncoated; top right, total thickness of coating 0.3 mm and width 9.2 mm; bottom left, total thickness 0.5 mm and width 9.2 mm; bottom right, total thickness 0.5 mm and width 11.2 mm.

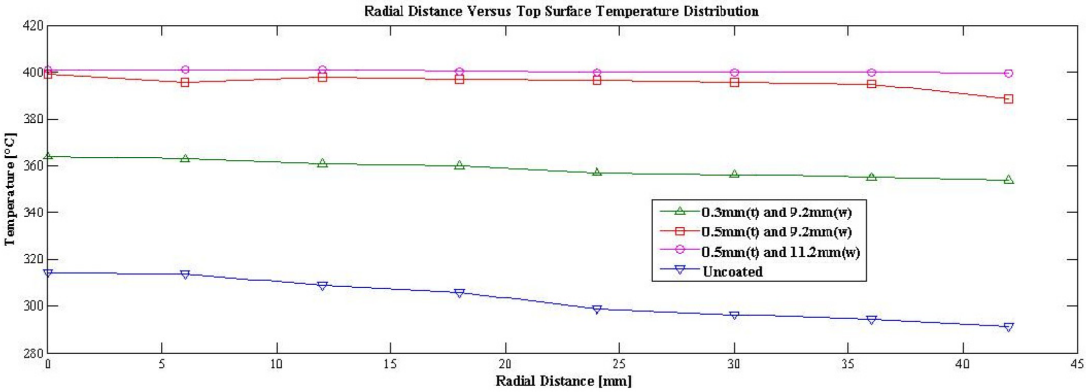

Figure 4. Temperature on the top surface as a function of radial distance.

5. Conclusions

FEM of an SI engine piston clearly shows that the piston's top surface temperature depends upon both ceramic coating thickness and width. The greatest increase in the maximum temperature of the top surface of the piston is almost 28% compared with the uncoated piston, while the piston's substrate temperature decreases, which together have a positive impact on the performance and efficiency of the engine.

References

1. Lima, C.R.C. & Guilemany, J.M. Adhesion improvements of thermal barrier coatings with HVOF thermally sprayed bond coats, *Surf. Coatings Technol.* **201** (2007) 4694– 4701.
2. Harris, D. & Lutz, J. Thermal barrier coatings—technology for Diesel engines. *SAE Trans.* **97** (Section 6: *Journal of Engines*) (1988).
3. Bleeks, T.W. & Graham, G.H. Chemical removal of ceramic thermal barrier and metallic bond coats from gas turbine combustion components (SAE Technical Paper 940053) (1994).
4. Novinski, E.R. The selection and performance of thermal sprayed abradable seal coatings for gas turbine engines (SAE Technical Paper 890929) (1989).
5. Chan, S.H. & Khor, K.A. The effect of thermal barrier coated piston crown on engine characteristics. *J. Mater. Engng Performance* **9** (2000) 103–109.
6. Rejda, E.F., Socie, D.F., Beardsley, M.B., Happoldt, P.G. & Kelley, K.C. Thermal barrier coatings for low emission, high efficiency diesel engine applications (SAE Technical Paper 1999-01-2255) (1999).
7. Vittal, M., Borek, J.A. & Boehman, A.L. The influence of thermal barrier coatings on the composition of diesel particulate emissions (SAE Technical Paper 972958) (1997).
8. Winkler, M.F. & Parker, D.W. Ceramic thermal barrier coatings provide advanced diesel emissions Control and improved management of combustion–exhaust system temperatures (SAE Technical Paper 931106) (1993).
9. Kahl, W.K. Thermal barrier effects on performance and emissions of a methanol fueled Dl engine (SAE Technical Paper 892163) (1989).
10. Dhananjaya, D.A., Mohanan, P. & Sudhir, C.V. Combustion and emission characteristics of diesel, B100 and B20 fuel on a thermal barrier coating on piston crown in direct injection C.I. engine at optimum IOP and IT (SAE Technical Paper 2009-28-0042) (2009).

11. Gilbert, A., Kokini, K. & Sankarasubramanian S. Thermal fracture of zirconia–mullite composite thermal barrier coatings under thermal shock: A numerical study. *Surf. CoatingsTechnol.* **203** (2008) 91–98.
12. Gilbert, A., Kokini, K. & Sankarasubramanian, S. Thermal fracture of zirconia–mullite composite thermal barrier coatings under thermal shock: An experimental study. *Surf. CoatingsTechnol.* **202** (2008) 2152–2161.
13. Muchai, J., Kelkar, A., Klett, D. & Jagannathan Sankar. Thermal–mechanical effects of ceramic thermal barrier coatings on Diesel engine piston. *MRS Proc.* **697** (2001) P8.10.
14. Hejwowski, T. & Weroński, A. The effect of thermal barrier coatings on diesel engine performance. *Vacuum* **65** (2002) 427–432.
15. Buyukkaya, E. Thermal analysis of functionally graded coating AlSi alloy and steel pistons. *Surf. Coatings Technol.* **202** (2008) 3856–3865.
16. Buyukkaya, E. & Cerit, M. Thermal analysis of a ceramic coating diesel engine piston using 3-D finite element method. *Surf. Coatings Technol.* **202** (2007) 398–402.
17. Ravindra Prasad & Samria, N.K. Heat transfer and stress fields in the inlet and exhaust valves of a semi-adiabatic diesel engine. *Computers Structures* **34** (1990) 765–777.
18. Parlak, A. & Ayhan, V. Effect of using a piston with a thermal barrier layer in a spark ignition engine. *J. Energy Inst.* **80** (2007) 223–228.
19. Cerit, M., Ayhan, V., Parlak, A. & Yasar, H. Thermal analysis of a partially ceramic coated piston: Effect on cold start HC emission in a spark ignition engine. *Appl. Thermal Engng* **31** (2011) 336–341.
20. Soyhan, H.S., Yıldırım, M., Karamangil, M.I., Sürmen, A. & Gül, Z. In-cylinder expansion of piston-ring crevice hydrocarbons in SI engines. 3rd Mediterranean Combustion Symp., June 2003, Morocco.
21. Marr, M.A. *An Investigation of Metal and Ceramic Thermal Barrier Coatings in a Spark-Ignition Engine* (M.S. thesis). University of Toronto (2009).
22. Cerit, M. Thermo-mechanical analysis of a partially ceramic-coated piston used in an SI engine, *Surf. Coatings Technol.* **205** (2011) 3499–3505.
23. Poola, R.B., Nagalingam, B. & Gopalakrishnan, K.V. Performance of thin ceramic-coated combustion chamber with gasoline and methanol as fuels in a two-stroke SI engine (SAE Technical Paper 941911) (1994).
24. Esfahanian, V., Javaheri, A. & Ghaffarpour, M. Thermal analysis of an SI engine piston using different combustion boundary condition treatments. *Appl. Thermal Engng* **26** (2006) 277–287.
25. Hohenberg, G.F. Advanced approaches for heat transfer calculations (SAE Technical Paper 790825) (1979).
26. Ma, W. & Dong, H. Ceramic thermal barrier coating materials. In: *Thermal Barrier Coatings* (eds Huibin Xu & Hongbo Guo), p. 27 (Table 2.1). Sawston: Woodhead (2011).
27. Praveen, K., Sivakumar, S., Ananthapadmanabhan, P.V. & Shanmugavelayutham, G. Lanthanum cerate thermal barrier coatings generated from thermal plasma synthesized powders. *Ceramics Intl* **44** (2018) 6417–6425.
28. Cao, X., Vassen, R., Fischer, W., Tietz, F., Jungen, W. & Stöver, D. Lanthanum–cerium oxide as a thermal barrier coating material for high-temperature applications. *Adv. Mater.* **15** (2003) 1438–1442.
29. Cerit, M. & Coban, M. Temperature and thermal stress analyses of a ceramic-coated aluminum alloy piston used in a diesel engine. *Intl J. Thermal Sci.* **77** (2014) 11–18.
30. Guo, H., Wang, Y., Wang, L. & Gong, S. Thermo-physical properties and thermal shock resistance of segmented $La_2Ce_2O_7$/YSZ thermal barrier coatings. *J. Thermal Spray Technol.* **18** (2009) 665–671.